Analysis of Real-Driving Data Variability for Connected Vehicle Diagnostics ⋆

Alvin Barbier * **José Miguel Salavert** * **Carlos E. Palau** *
Carlos Guardiola *

* *Universitat Politècnica de València, Camino de Vera s/n, E-46022*
Valencia, Spain (e-mail: {albar9,carguaga}@upv.es)

Abstract: Connected vehicle paradigm allows the systematic recording of data, which may be made available for both on-board and cloud diagnostics functions. However, real-driving conditions may be highly dynamic, making the application of diagnostic methods cumbersome. This article analyzes the variability of real-world data coming from a mild hybrid vehicle at various levels (i.e., vehicle, powertrain and engine cycle). The results show that although non-steady, real-driving conditions can exhibit situations that could be leveraged to characterize the nominal operation of the vehicle over time and therefore ease the detection of faulty operation.

Keywords: Real-driving conditions, data-driven diagnostic, in-cylinder pressure, connected vehicle

1. INTRODUCTION

The increasing number of actuators, sensors and control strategies embedded in modern vehicles have allowed manufacturers and OEMs to comply with the evolving emissions legislation (Payri et al., 2015). At the same time, this also had the effect to increase the complexity of the vehicles architecture and therefore the risk of faulty operation (Zhang et al., 2009). Yet, the larger number of sensors in the vehicles offers a better diagnostic capability (Kiencke and Nielsen, 2005). Current on-board diagnostics (OBD) monitor a plethora of variables and aim to detect early on faults to notify the driver that a maintenance operation is required (Saibannavar et al., 2021).

Current solutions in the automotive industry traditionally lack of ability to monitor, analyze and compare data over the vehicle's lifespan. Recent advancements in technologies and vehicles connectivity provide however for a whole new perspective for vehicles diagnostics (Guardiola et al., 2021b). Either embedded in the vehicle or computed remotely, the knowledge resulting from the systematic recording of real-world operation data will enable improvements in faults detection and diagnostic models. Pattern recognition and prediction (Joud et al., 2020; Luján et al., 2021), machine learning algorithms (Garg et al., 2021), big data and internet of things (IoT) (Maksimychev et al., 2021; Meenakshi et al., 2021), are all examples of applications that have gained interest in the recent years to leverage the quantity of data made available.

Many diagnostic strategies are based on outliers detection and residuals analysis. For example, Kimmich et al. (2005) were able to detect faults in the intake and the injection systems thanks to residuals measurement. After characterizing nominal operation with models, Jung (2019) developed a classifier based on the measured residuals to identify and separate different faults. These examples show that the correct execution of data-driven diagnostic methods is, somewhat, reliant on the characterization of the nominal fault-free operation of the system. In particular, characterizing the expected variation of a given quantity under specific conditions is required. From a transportation perspective, this characterization can be established at various levels: from fleet, to vehicle, and down to component level (Guardiola et al., 2021b).

In internal combustion engine vehicles, modern engine control units (ECU) integrate sufficient computational power to deal with high speed analog signals acquisition and real-time execution, which provides effective diagnostic and control capabilities at various components and subsystems levels (Reif, 2014). Combustion diagnostic itself traditionally relies on knock sensors and instantaneous engine speed calculation from crankshaft position measurement (Lee et al., 2001; Guillemin et al., 2008). Although cost-effective and non-intrusive, these approaches do not provide a direct measurement of the cylinder conditions. However, the need for robust performance and diagnostic in real-driving conditions, in order to comply with the legislation over the vehicle's lifespan, could require a more accurate solution. Usually limited to research activities, the in-cylinder pressure sensor has found some applications in production engines (Hadler et al., 2008; Kazuhiro et al., 2017). This sensor offers the opportunity to obtain a direct measurement of the combustion process and exhibits the potential to be implemented in a large number of observation and control applications (Willems, 2018; Guardiola et al., 2021a).

This article aims to analyze data registered from a vehicle in real-driving conditions. Compared to a controlled environment such as in engine test bench experiments, real-world operation is subject to many external disturbances.
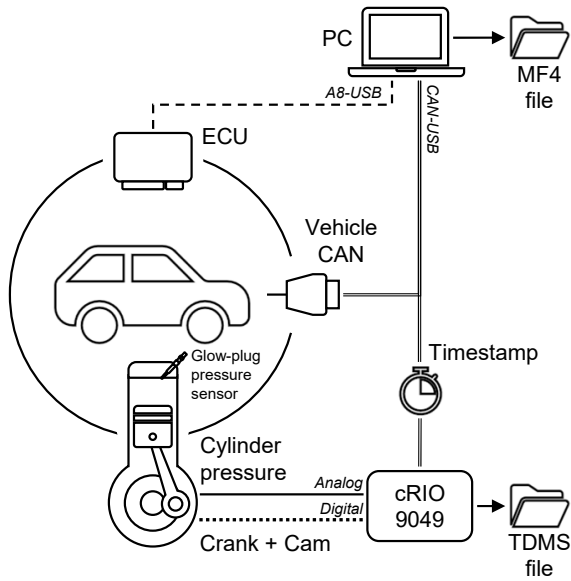
Fig. 1. Systems communication and data acquisition layout.

The nominal operation might consequently be affected and the expected variation of the data must be analyzed. By doing so, one could compare if the levels measured during the research and development process can be expected in the final implementation. Such analysis can be done at different levels (e.g., fleet, vehicle, powertrain operation) and in this work the crank-based combustion evolution itself was also considered. To the best of the authors knowledge, such measurement and analysis has not been extensively performed in real-world conditions. The paper is organized as follows: first, the experimental setup is presented. Section 3 describes some considerations regarding the acquisition and processing of the data and section 4 presents the results of the analysis. Finally, section 5 summarizes the findings of this article.

2. EXPERIMENTAL SETUP

The database studied in this work consisted in everyday life trajectories from a mild hybrid diesel C-segment vehicle. Data were gathered from various sources and a special attention had to be dedicated to the processing of these data. Figure 1 shows a scheme of the global systems communication layout. Different layers with different objectives can be found.

At the vehicle level, information provided by the ECU (e.g., injection settings) and the vehicle CAN network were transmitted to a laptop (PC) in charge of gathering the incoming data. The communication from the ECU to the PC was made possible by the A8 serial interface where ATI Vision software was used to access the calibration and data acquisition. The vehicle CAN bus was connected to the PC via a CAN to USB interface. Over 250 measurement channels were recorded in this setup, including ECU sensors and actuators, and vehicle sensors such as GPS. Data from the ECU and the CAN bus were stored on a single MF4 file.

The engine was equipped with an OPTRAND AutoPSI-TC in-cylinder pressure sensor integrated in one of the

engine glow-plugs. Engine test bench applications traditionally rely on research encoders with a tuned resolution to provide the acquisition frequency. In this case, the 60-2 crank trigger wheel signal was used instead. The acquisition of this signal was carried out by a real-time cRIO-9049 from NI where a NI-9401 digital module was used to measure the edges provided by such signal. The 60-2 crank signal represents, however, a low sampling frequency clock for a proper in-cylinder pressure acquisition. A software clock divider was therefore used in order to generate a virtual encoder with a final resolution of 0.375 crank angle degree (CAD). This calculation was performed in the field-programmable gate array (FPGA) embedded in the cRIO-9049 and the resulting crank-angle *clock* signal was used to define the acquisition of the in-cylinder pressure, whose signal was measured by a 16 bits resolution NI-9223 analog acquisition module. Finally, in order to calculate the cycle-to-cycle combustion metrics, the acquisition of the in-cylinder pressure requires to be referenced with the crankshaft position. Here, the 60-2 trigger signal together with the camshaft position signal were used to get the piston position (Reif, 2014). In-cylinder pressure data acquisition and processing were programmed on the real-time system, which streamed all data to a disk in TDMS format, and published cycle metrics plus a clock time stamp on the CAN network via a NI-9853 CAN module.

3. METHODOLOGY

3.1 Acquisition, update and phasing of the data

As described in the previous section, the present experimental setup makes use of various data sources. Such configuration is therefore characterized by different update and acquisition rates depending on the considered system. In this case, ATI Vision was used for registering the relevant ECU channels every 10 ms. Vehicle CAN network messages were recorded when available, thus resulting in a variable acquisition frequency. This was significantly relevant for in-cylinder pressure metrics, which were updated once per cycle. This means that, along the experiment, the data might be updated and acquired at different moments, as illustrated in Figure 2. In this figure, the black dot markers correspond to the acquisition time steps of the ECU variables, the orange dots are the update of the combustion calculations and acquisition made by the cRIO-9049, and the blue diamonds represent the update rate of the vehicle CAN variables whose value varies depending on the selected variables.

From the ATI Vision side, every variable acquired is paired with a time stamp in order to phase them over time in the data processing. That is, when starting to save the data, a time vector is incremented and once a variable is acquired, either from the ECU or the CAN bus, the corresponding time stamp is saved as well. As previously mentioned, the data saved by the cRIO do not share the same time vector increment than the MF4 file. Consequently, the cRIO time stamp at which the engine cycle is computed and saved is also sent by CAN to the PC and serves as the reference to phase the signals afterwards.

This experimental setup aims to compare data coming from the vehicle on an engine cycle-to-cycle basis. Therefore, it was decided to discretize and phase the signals
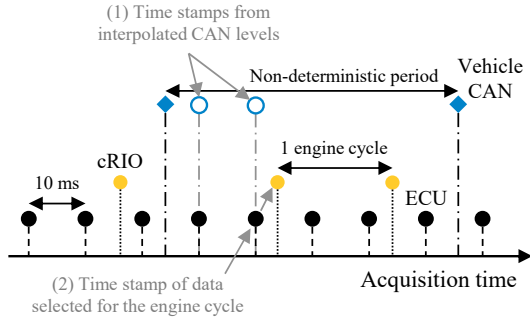
Fig. 2. Update and acquisition time steps (markers) of the different systems along the experiment. *Not to scale representation.*

accordingly. Although various ways to achieve it might be possible, here, the following methodology was selected (indications in grey in Figure 2 illustrate these steps):

(1) Firstly, the values coming from the CAN bus (e.g., vehicle GPS coordinates) were interpolated according to the ECU acquisition time steps in order to process the data from these two sources in the same time basis. That is, CAN levels are linearly interpolated at every ECU time step using the nearest CAN information.

(2) Secondly, at every engine cycle, the corresponding cRIO-9049 time stamp, saved through CAN, is sought in the MF4 file. Once encountered, the previous nearest time stamp of the ECU is selected and the corresponding ECU and interpolated vehicle CAN values are associated to the engine cycle. In the case where both the engine cycle and ECU acquisition occur at the same time, then they are directly associated. Note that this approach might imply a cycle delay sometimes because it is never certain whenever the engine cycle will be saved and when the actual change in the ECU settings occur. Yet, it was found that this strategy was providing sufficiently phased signals to conclude on a cycle-to-cycle analysis.

3.2 In-cylinder pressure processing

The in-cylinder pressure signal requires some processing in order to analyze the combustion evolution (Payri et al., 2010). First, the signal was leveled (*pegging*) with the intake manifold pressure near the intake bottom dead center (BDC) (Brunt and Pond, 1997). Then, the signal was filtered at 1500 Hz to remove the resonant frequencies content (Guardiola et al., 2018).

In this article, the gross indicated mean effective pressure (IMEP) was used as an indicator of the engine load and its value was obtained with the following equation:

$$IMEP = \frac{1}{V_d} \int_{BDC_1}^{BDC_2} p \, dV \tag{1}$$

where V_d is the engine cylinder displacement volume, p the in-cylinder pressure, V the instantaneous combustion chamber volume obtained from geometric crankshaft-piston position, and the limits of the integration are the compression and the expansion bottom dead centers, BDC_1 and BDC_2 respectively.
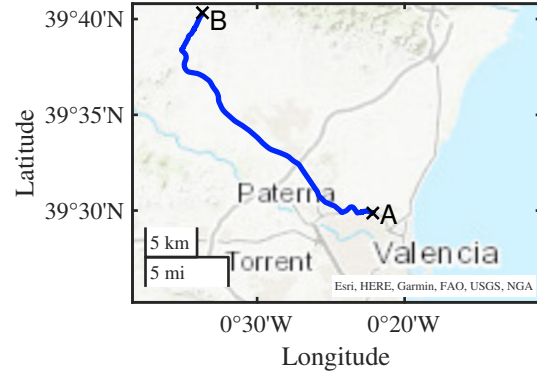

Fig. 3. Geographical location of the selected vehicle trajectory.

One important tool when analyzing the evolution of the combustion is the heat release calculation. Here, as no significant accuracy was required, the apparent heat release computation with a constant polytropic coefficient was used (Asad and Zheng, 2008):

$$dQ = \frac{\kappa}{\kappa - 1} p \, dV + \frac{1}{\kappa - 1} V \, dp \tag{2}$$

with κ the polytropic coefficient set to 1.3

4. RESULTS AND DISCUSSION

In the considered setup, characterizing the nominal operation can be done at various levels: vehicle and powertrain operation, and combustion evolution. In the first one, the registered data could allow to characterize and model quantities under nominal operating conditions in order to detect any deviation over time (e.g., NO_x emissions to detect sensor drift or abnormal combustion). Also, having access to historic data, one could characterize the speed profile at a specific location in order to get knowledge about the driving style, eventual traffic conditions, expected fuel consumption, etc. In the second category, thanks to the access to the in-cylinder pressure evolution, one could analyze if the combustion is similar between cycles with the same injection settings, get a direct measurement of the load through IMEP calculation, build in-cylinder pressure process models, etc. The case studies are various and in this work some examples were selected to analyze how the nominal operation of various quantities could be characterized from real-world data provided with such experimental setup.

From a vehicle point of view, it was first decided to analyze the database available in this study. Most of the data recorded come from the high speed-low acceleration range, corresponding to highway conditions. Accordingly, a recurrent trajectory from the database with a highway section was found and selected. This trajectory, illustrated in blue from point A to point B in Figure 3, was performed in the area of the city of Valencia (Spain) and includes mostly extra-urban and highway conditions. Such situation might also be found at a fleet level considering that most of the vehicles experience a recurrent trajectory (e.g., commuting from home to workplace and vice versa).
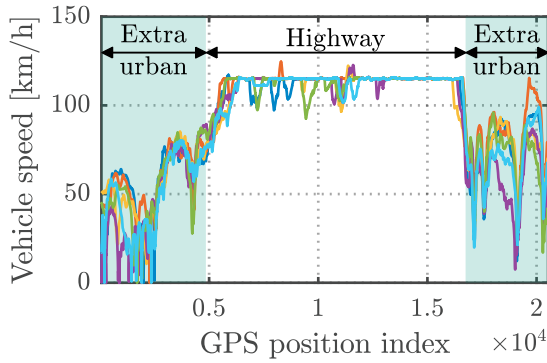
Fig. 4. Evolution of the vehicle speed at various days of experiments along the same recurrent trajectory.

Considering that the selected trajectory passes through the same GPS coordinates, it could be of interest to compare the speed levels over time at the same location to characterize the nominal operation of the vehicle. Figure 4 shows the monitored vehicle speed at the various days of experiments (note that for a better readability and interpretation of the results, here the x-axis corresponds to a specific latitude-longitude location transcribed into a single sample index). It can be observed that real-driving conditions, especially for urban and extra-urban areas, are highly impacted by the traffic conditions. Nonetheless, as observed in the last part of the highway segment, it is still possible to detect some areas with very similar conditions which might be of a better candidate for a nominal operation characterization.

Figure 5 shows the vehicle speed profile from each test at the end part of the highway segment from Figure 4 where the traffic conditions allowed to obtain similar results. Note that in these tests, the driver was enabling the vehicle cruise control on highway conditions which is believed to have greatly participated into obtaining similar profiles. Indeed, compared to pedal control from the driver, the cruise control strategy is expected to be more prone to provide similar speed profiles at the same GPS location. It can be seen that the cruise control strategy exhibited quite a repetitive behavior which resulted in very similar vehicle speeds for a same GPS location (in this segment the mean vehicle speed standard deviation between experiments was about 0.07 km/h). Once these conditions are established, it is then possible to compare other metrics from the vehicle. As an example, once could build a *nominal operating conditions* model with a confidence interval for vehicle speed and other metrics such as the injected fuel quantity. In this particular case, the solid black lines in this figure represent such hypothetical envelope that could be characterized under normal engine operation mode. In the bottom plot, around the end of the selected segment, it is observed that in one of the experiments an abrupt increase in the injected fuel quantity occurs and exits the nominal interval. Although the fuel quantity value might be expected to vary with vehicle's attributes such as the total vehicle payload, or external disturbances such as wind conditions, in this case this was justified by a change in the combustion mode due to a regeneration of the diesel particulate filter (DPF). In the case where no variation in the combustion mode would have occurred, such deviation from the confidence interval might have been detected
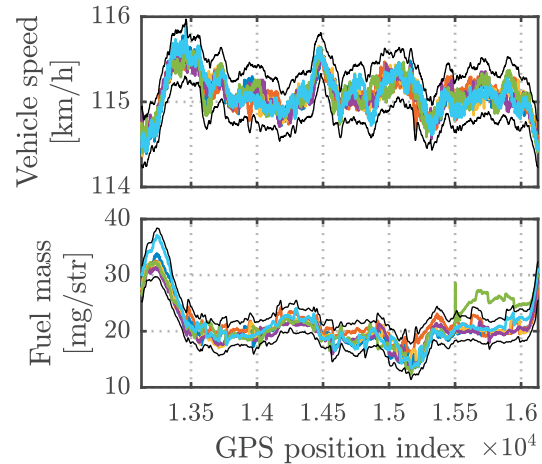

Fig. 5. Zoom on a segment (highway) from the trajectory where the vehicle speed (top) was detected to be in the same range for all the experiments. The respective fuel quantity injected is shown in the bottom plot. The solid black lines represent a hypothetical model confidence interval.

thanks to the recording of the vehicle's data over time and therefore trigger a fault detection.

The previous example was limited to quasi-steady conditions in terms of vehicle speed, which helped to characterize the nominal operation of the vehicle from this point of view. However, as previously observed in Figure 4, real-driving conditions are made of significant transients. Nonetheless, the characterization of the nominal operation of the system might be performed at another scale where no steady operation is required. Following the previous observation made on the injected fuel quantity, thanks to the measurement of the in-cylinder pressure it is possible to calculate the IMEP (i.e., the engine load) in a cycle-to-cycle basis. This value is expected to be well correlated with the quantity of fuel injected in the cylinder. Figure 6 shows the measured IMEP against the total injection quantity set by the injection strategy in the ECU for the whole database filtering out the non-normal engine modes (e.g., DPF regeneration). This figure shows the distribution of around 1.5 million cycles where the brightest region shows the highest density. The darkest regions correspond to low density cycles and are explained by the eventual cycle delay resulting from the phasing of the data as explained in section 3, especially for the low load-low fuel quantity region due to recurrent pedal tip-in/tip-out. Nonetheless, a fairly clear relationship and model between fuel quantity and IMEP under nominal operation could be inferred from the database. Such characterization could then help to detect any injector fault or abnormal combustion conditions by detecting various cycles outside of a confidence interval, e.g., injectors performance worsening due to coking (D'Ambrosio and Ferrari, 2012).

The present experimental setup offers the potential to diagnose the engine operation at a deeper and higher resolution level than vehicle and powertrain operation thanks to the crank-based measurement of the in-cylinder pressure signal. Either from a diagnostic or modeling and prediction perspective, the repeatability of the combustion under similar operating conditions is essential. Engine
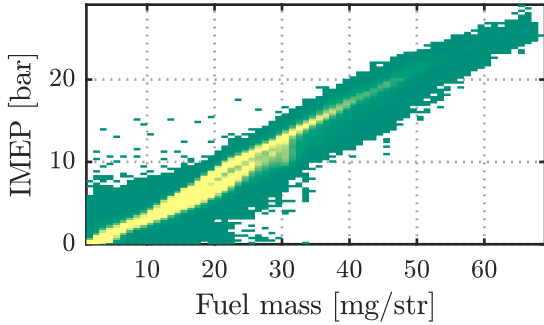
Fig. 6. Density plot of the relation between the quantity of fuel set by the ECU and the corresponding IMEP measured from in-cylinder pressure.

test bench research activities are able to characterize the nominal engine cyclic variability thanks to steady-state conditions and long settling times. However, as previously observed, real-driving conditions do not exhibit long periods of steady conditions and instead are prone to dynamic operation that might affect the cyclic variability. Yet, it is believed that at different moments of the vehicle's usage, various cycles should be monitored at similar operating conditions. Within the available database, cycles with the same injection settings and engine speed from all the experiments were sought and two datasets were selected, see Figure 7. In particular, two types of conditions were chosen: *steady* and *transient*. As illustrated in the top plot of Figure 7, one dataset was created from cycles occurring in a relatively steady operation with low acceleration profiles (e.g., highway), while the other one corresponds to a more dynamic situation. Note that all the cycles are not represented in the top plot (only for illustration purposes). This figure shows: the cycle-to-cycle in-cylinder pressure (p_{cyl}) and heat release rate (dQ) traces from the two selected operating conditions in grey, as well as an average cycle in black. In the middle plot, the average injector's signal is also shown in blue for illustration purposes (maximum start of injections and injection quantities standard deviation from all the cycles are 0.015 CAD and 0.06 mg/str, respectively). The results from this cycle analysis can be found in Table 1. It can be appreciated that some cycles with similar injection settings and operating conditions might be detected and allow therefore to characterize the cyclic variability from real-driving conditions. Here, the maximum in-cylinder pressure value and position, as well as the maximum heat release rate value and position, were arbitrarily chosen as indicators to evaluate the cyclic variability of these signals, as listed in Table 1. Note that the values provided for the crank angle positions of these metrics are given according to the resolution of the virtual encoder (i.e., 0.375°) and that their values are expressed in degrees after the top dead center (aTDC). From these results, it is observed that some repeatability can be found even from an engine cycle level although measured from different experiments. These variability levels could be compared to engine test bench results, used to build models of the engine in real-driving conditions, or kept as a reference and therefore ease the detection of faulty operation by comparing these traces with future ones.
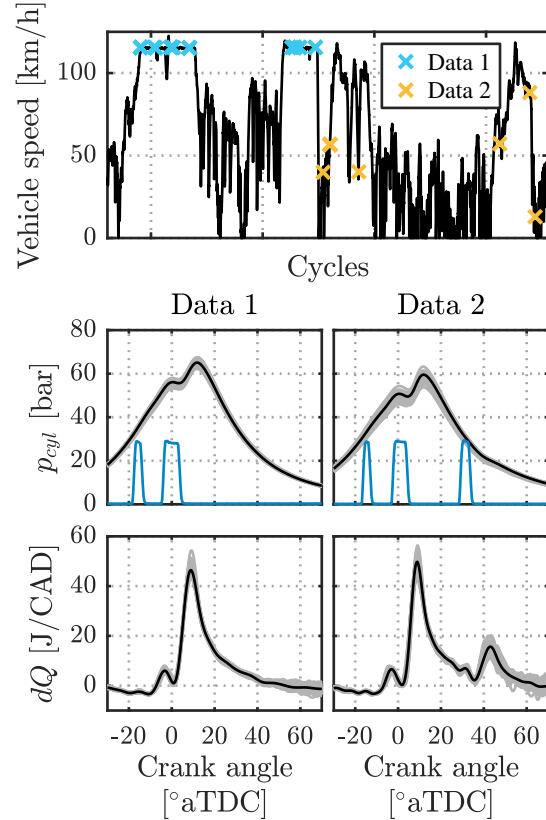

Fig. 7. Selection of two cycles datasets in different driving conditions (top). The in-cylinder pressure (middle) and heat release rate (bottom) traces from all the cycles are shown in grey and an average cycle is shown in black. An average injector signal (middle) is illustrated in blue.

Table 1. Operating conditions and results of the cyclic variability analysis from Figure 7 ($\overline{x}$: mean value, σ_x: standard deviation).

Variable (x)		Data 1 (248 cycles)		Data 2 (137 cycles)	
		$\overline{x}$	σ_x	$\overline{x}$	σ_x
n	[rpm]	2079	2.7	1590	5.9
m_f	[mg/str]	15.15	0.05	19.65	0.07
p_{rail}	[bar]	729	5.5	471	9.4
p_{int}	[bar]	1.33	0.02	1.24	0.06
T_{int}	[°C]	45	3	41.6	3
T_{cool}	[°C]	90.7	7.5	88.7	6.2
r_{EGR}	[%]	25.5	1.2	26.7	4
p_{cyl}^{max}	[bar]	65.08	1.09	59.73	1.80
$\theta\left(p_{cyl}^{max}\right)$*	[°aTDC]	12	0.190	12	0.174
dQ_{max}	[J/CAD]	45.58	2.11	50.46	2.87
$\theta(dQ_{max})$*	[°aTDC]	9.00	0.181	8.625	0.251

n: engine speed, m_f: fuel quantity, p_{rail}: rail pressure, p_{int}: intake manifold pressure, T_{int}: intake manifold temperature, T_{cool}: engine coolant temperature, r_{EGR}: exhaust gas recirculation rate, θ: crank angle position
*Note that the σ_x value might be below the virtual encoder resolution (0.375°) and this value should therefore be considered with care.

5. SUMMARY AND CONCLUSIONS

The increase in vehicles connectivity has the potential to extend the diagnostics capabilities beyond the boundaries encountered up to now. Still, it remains important to leverage the amount of data generated by the vehicles and to evaluate their capacity to transmit the information intended to the desired application. Many diagnostic methods rely on some sort of outliers detection. To do so, *nominal operation* must be characterized at first. This paper proposed to analyze some use cases for characterizing such nominal operation at various levels: vehicle, powertrain and combustion. The database used in this work was based on real-world driving conditions from an instrumented vehicle. Starting from highway cruise control conditions, various experiments from a recurrent trajectory were found to exhibit very similar speed profiles at the same GPS location. By harnessing this situation at a deeper level, it was found that a nominal operation speed and fuel quantity interval could be inferred and participate in detecting faulty injections. Finally, the analysis was oriented towards high resolution signals such as in-cylinder pressure and heat release rate by evaluating the cyclic variability over various experiments with the same injection settings in real-driving conditions. The results illustrated that characterizing the system could be made at various levels, which should participate significantly in improving embedded and remote diagnostic methods for real-driving conditions by considering availability of historic data from the vehicle.

REFERENCES

Asad, U. and Zheng, M. (2008). Fast heat release characterization of a diesel engine. *International Journal of Thermal Sciences*, 47(12), 1688–1700.

Brunt, M.F.J. and Pond, C.R. (1997). Evaluation of Techniques for Absolute Cylinder Pressure Correction. *SAE Technical Paper*.

D'Ambrosio, S. and Ferrari, A. (2012). Diesel Injector Coking: Optical-Chemical Analysis of Deposits and Influence on Injected Flow-Rate, Fuel Spray and Engine Performance. *Journal of Engineering for Gas Turbines and Power*, 134(6), 062801.

Garg, P., Silvas, E., and Willems, F. (2021). Potential of machine learning methods for robust performance and efficient engine control development. In *IFAC-PapersOnLine*, volume 54, 189–195. Elsevier B.V.

Guardiola, C., Pla, B., Bares, P., and Barbier, A. (2018). An analysis of the in-cylinder pressure resonance excitation in internal combustion engines. *Applied Energy*, 228, 1272–1279.

Guardiola, C., Pla, B., Bares, P., and Barbier, A. (2021a). Individual cylinder fuel blend estimation in a dual-fuel engine using an in-cylinder pressure based observer. *Control Engineering Practice*, 109(January), 104760.

Guardiola, C., Vigild, C., de Smet, F., and Schusteritz, K. (2021b). From OBD to connected diagnostics: A game changer at fleet, vehicle and component level. *IFAC-PapersOnLine*, 54(10), 558–563.

Guillemin, F., Grondin, O., Chauvin, J., and Nguyen, E. (2008). Combustion Parameters Estimation Based on Knock Sensor for Control Purpose Using Dedicated Signal Processing Platform. In *SAE Technical Papers*, volume 2008.

Hadler, J., Rudolph, F., Dorenkamp, R., Stehr, H., Hilzendeger, J., and Kranzusch, S. (2008). Volkswagen's new 2.0 l TDI engine for the most stringent emission standards — Part 1. Technical Report 5.

Joud, L., Da Silva, R., Chrenko, D., Kéromnès, A., and Le Moyne, L. (2020). Smart Energy Management for Series Hybrid Electric Vehicles Based on Driver Habits Recognition and Prediction. *Energies*, 13(11), 2954.

Jung, D. (2019). Engine Fault Diagnosis Combining Model-based Residuals and Data-Driven Classifiers. *IFAC-PapersOnLine*, 52(5), 285–290.

Kazuhiro, N., Atsushi, I., Kota, M., Takashi, K., Toru, M., and Takashi, Y. (2017). Control device for compression ignition-type engine. U.S. Patent No. 9,719,441 B2.

Kiencke, U. and Nielsen, L. (2005). *Automotive Control Systems: For Engine, Driveline, and Vehicle*. Springer Berlin Heidelberg, Berlin, Heidelberg.

Kimmich, F., Schwarte, A., and Isermann, R. (2005). Fault detection for modern Diesel engines using signal- and process model-based methods. *Control Engineering Practice*, 13(2), 189–203.

Lee, B., Rizzoni, G., Guezennec, Y., Soliman, A., Cavalletti, M., and Waters, J. (2001). Engine Control Using Torque Estimation. In *SAE Technical Papers*.

Luján, J.M., Pla, B., Bares, P., and Pandey, V. (2021). Adaptive calibration of Diesel engine injection for minimising fuel consumption with constrained NOx emissions in actual driving missions. *International Journal of Engine Research*, 22(6), 1896–1905.

Maksimychev, O., Matiukhina, E.N., Ostroukh, A.V., and Vasiliev, Y.E. (2021). Connected Vehicle Remote Diagnostic System. In *2021 Systems of Signals Generating and Processing in the Field of on Board Communications*, 1–5. IEEE.

Meenakshi, Nandal, R., and Awasthi, N. (2021). OBD-II and Big Data: A Powerful Combination to Solve the Issues of Automobile Care. In *Advances in Intelligent Systems and Computing*, volume 1257, 177–189.

Payri, F., Luján, J.M., Martán, J., and Abbad, A. (2010). Digital signal processing of in-cylinder pressure for combustion diagnosis of internal combustion engines. *Mechanical Systems and Signal Processing*, 24(6), 1767–1784.

Payri, F., Luján, J., Guardiola, C., and Pla, B. (2015). A Challenging Future for the IC Engine: New Technologies and the Control Role. *Oil & Gas Science and Technology – Revue d'IFP Energies nouvelles*, 70(1), 15–30.

Reif, K. (2014). *Diesel Engine Management*. Springer Fachmedien Wiesbaden, Wiesbaden.

Saibannavar, D., Math, M.M., and Kulkarni, U. (2021). A Survey on On-Board Diagnostic in Vehicles. In *EAI/Springer Innovations in Communication and Computing*, 49–60.

Willems, F. (2018). Is Cylinder Pressure-Based Control Required to Meet Future HD Legislation? *IFAC-PapersOnLine*, 51(31), 111–118.

Zhang, Y., Gantt, G., Rychlinski, M., Edwards, R., Correia, J., and Wolf, C. (2009). Connected Vehicle Diagnostics and Prognostics, Concept, and Initial Practice. *IEEE Transactions on Reliability*, 58(2), 286–294.